FINITE DEFLECTIONS OF A SIMPLY SUPPORTED RIGID-PLASTIC CIRCULAR PLATE LOADED DYNAMICALLY

N. JONES

20060110152

FINITE DEFLECTIONS OF A SIMPLY SUPPORTED RIGID-PLASTIC

CIRCULAR PLATE LOADED DYNAMICALLY*

by

Norman Jones

Division of Engineering
Brown University
Providence, Rhode Island

May 1967

Finite Deflections of a Simply Supported Rigid-Plastic

Circular Plate Loaded Dynamically

by

Norman Jones*

Abstract

A theoretical analysis is presented for the dynamic behavior of a simply supported rigid, perfectly plastic circular plate subjected to a rectangular pressure pulse. It is shown that this theory, which considers the simultaneous influence of membrane forces and bending moments, predicts final deformations which are considerably smaller than those given by the corresponding bending theory of Hopkins and Prager even when maximum deflections only of the order of the plate thickness are permitted. It is believed that this theoretical analysis should assist in the interpretation of the dynamic biaxial stress-strain characteristics of materials recorded on diaphragms fitted in impact tubes and could be developed further in order to describe the behavior of plates having other support conditions and different dynamic loading characteristics.

---

* Assistant Professor of Engineering (Research), Division of Engineering, Brown University.

Notation

H	plate thickness
I	impulse per unit area of plate
I'	$\dfrac{I}{(\mu H p_o)^{1/2}}$
M_o	$\sigma_o H^2/4$
M_r, M_θ	radial and circumferential bending moments per unit length
N_o	$\sigma_o H$
N_r, N_θ	radial and circumferential membrane forces per unit length
Q	transverse shear force per unit length of plate
R	outside radius of plate
R_r, R_θ	principal radii of curvature
T	time at which plate reaches permanent position
k(t), k_o	uniform distributed pressure per unit area of undeformed plate
m_r, m_θ	dimensionless bending moments M_r/M_o, M_θ/M_o
n_r, n_θ	dimensionless membrane forces N_r/N_o, N_θ/N_o
p	$-k \sin\phi$
p_o	$\dfrac{6M_o}{R^2}$
q	$-k \cos\phi$
r	radial coordinate of plate
t	time
u	displacement in direction r of undeformed plate
w	transverse deflection perpendicular to undeformed plate

Notation (continued)

x	r/R
y	ρ/R
y_o	ρ_o/R
α_r	$1 + \epsilon_r$
α_θ	$u + r$
γ	$\left(\dfrac{4p_o}{\mu H}\right)^{1/2}$
δ	$-2p_o/\mu$
$\epsilon_r,\ \epsilon_\theta$	radial and circumferential strains
θ	circumferential coordinate lying in plate
$\kappa_r,\ \kappa_\theta$	radial and circumferential curvatures
λ	k_o/p_o
μ	mass per unit area of plate
$\rho,\ \rho_o$	radius of hinge circle
σ_o	yield stress in simple tension
τ	duration of pulse
ϕ	slope of the mid-plane of a plate measured in a plane which passes through $r = 0$ and is perpendicular to the plate surface
$\dot{(\ )}$	$\dfrac{\partial}{\partial t}(\ )$
$(\ )'$	$\dfrac{\partial}{\partial r}(\ )$

1. Introduction

The behavior of rigid-plastic circular plates under the influence of static loads which produce infinitesimal deflections is fairly well established [1, 2, 3, etc.]. When finite deflections are permitted, however, it is observed that plates can support external loads considerably larger than those predicted by these theories. Onat and Haythornthwaite [4] indicated that this increased load carrying capacity is due mainly to the important role which membrane forces play in the finite deformation of plates.

It is clear from a survey of the pertinent literature that most attention has been directed towards the dynamic deformation of plates in which either membrane forces [5, 6, etc.] or bending moments [7, 8, 9, etc.] alone are believed to be important. Moreover, with the exception of some numerical work [10], the analysis of an annular plate by Florence [11], and some recent work [12], no investigations have been conducted into the interaction effects between membrane forces and bending moments, although such interaction influences considerably the static loading of plates [4] and the dynamic loading of beams [13]. Florence [14] applied uniform distributed impulses to some simply supported circular plates and observed that the appropriate rigid-plastic theory [8] overestimated considerably the recorded deflections particularly for large impulses. Recently it has been demonstrated [12] that a significant improvement in the theoretical predictions of plates loaded impulsively can be achieved if the influence of membrane forces and bending moments is retained in the theory.

Symonds [15] indicated that the permanent deformation of rigid-plastic beams subjected to central force pulses having rectangular and triangular shapes differed about ±15% from an equivalent half sine wave pulse with the same maximum value and impulse. Perzyna [16] developed further the theory of Hopkins and Prager [7], in which membrane forces are disregarded, and showed that for a given impulse the character of the pressure-time function had little influence on the final shape of a rigid-plastic circular plate. Hodge [17] and Sankaranarayanan [18], on the other hand, found that the blast characteristics had a profound effect upon the final deformation of cylindrical and spherical rigid-plastic shells.

In practice, the blast load which acts on a plate or structure often persists for a short period of time rather than behaving like a pure impulse as assumed in Ref. [12]. It is the purpose of this article, therefore, to study the behavior of a rigid, perfectly plastic circular plate when subjected to a rectangular pressure pulse such as the one shown in Fig. 1. The results of this analysis will be compared with the corresponding values from Ref. [7] so that they indicate the importance of membrane forces and with those of Ref. [12] in order to examine and assess the difference between the permanent deflections corresponding to a pure impulse and an equivalent rectangular pressure pulse.

2. Equilibrium Equations

It may be shown that the equilibrium equations for the finite deflections of a circular plate subjected to axisymmetrical dynamic loads can be written in the form [12]

$$(\alpha_\theta N_r)' - \alpha_\theta' N_\theta - \alpha_r \alpha_\theta Q/R_r + \alpha_r \alpha_\theta p + \mu \alpha_\theta \ddot{w} \sin\phi - \mu \alpha_\theta \alpha_\theta' \ddot{u} \cos\phi = 0 \qquad (1)$$

$$(\alpha_\theta Q)' + \alpha_r \alpha_\theta [N_r/R_r + N_\theta/R_\theta] + \alpha_r \alpha_\theta q + \mu \alpha_\theta \alpha_\theta ' \ddot{w} \cos\phi + \mu \alpha_\theta \ddot{u} \sin\phi = 0 \qquad (2)$$

$$(\alpha_\theta M_r)' - \alpha_\theta ' M_\theta - \alpha_r \alpha_\theta Q = 0 \qquad (3)$$

provided the rotary inertia effect is disregarded, and

$$\alpha_r = 1 + \epsilon_r$$

$$\alpha_\theta = r + u = r(1 + \epsilon_\theta)$$

$$1/R_r = \phi'/(1 + \epsilon_r)$$

$$1/R_\theta = \sin\phi/r$$

The positive directions of the various quantities are indicated in Fig. 2.

If we limit our discussion to plates having small strains and deflections which are not too large, then we may let $\alpha_\theta = r$, $\alpha_r = 1$, $1/R_r = \phi'$, $1/R_\theta = \sin\phi/r$, and $\alpha_\theta ' = \cos\phi$ which, using $\cos\phi = 1$, and $\sin\phi = -w'$, allow equations (1)-(3) to be recast as follows

$$rn_r' + n_r - n_\theta = -rkw'/N_o + \mu r\ddot{w}w'/N_o + \mu r\ddot{u}/N_o \qquad (4)$$

and

$$rm_r'' + 2m_r' - m_\theta ' - 4n_\theta w'/H = rk/M_o - \mu r\ddot{w}/M_o + \mu r\ddot{u}w'/M_o \qquad (5)$$

where,

$$n_{r,\theta} = N_{r,\theta}/N_o$$

$$m_{r,\theta} = M_{r,\theta}/M_o$$

and $r\phi'Q$, $rN_r\phi'$ and $\phi'w'$ have been disregarded.

3. Strains and Curvatures

It may be shown for small strains [19] that

$$\dot{\epsilon}_r = (1 + u')\dot{u}' + w'\dot{w}' \qquad (6)$$

$$\dot{\epsilon}_\theta = \dot{u}/r \qquad (7)$$

$$\dot{\kappa}_r = (1 + u')\dot{w}'' + \dot{u}'w'' - \dot{u}''w' - u''\dot{w}' \qquad (8)$$

and

$$\dot{\kappa}_\theta = \dot{w}'/r \qquad (9)$$

Griffith and Vanzant [20] observed that the material of a circular plate tends to move in a transverse sense at high rates of dynamic loading. This suggests that

$$u = 0 \qquad (10)$$

4. Yield Condition

It has been found that disregarding elastic effects when analyzing cantilever beams loaded dynamically is a powerful simplification and a valid approximation, provided the external energy is at least three times larger than the strain energy absorbed by the beam at the elastic limit [21]. Further, Frederick [5] and Boyd [6] investigated the deformation of membranes made from work-hardening material and found that a simplified perfectly plastic analysis provided a remarkably accurate model of the true behavior. Consequently the plate shown in Fig. 2 is assumed for the purposes of this analysis to be made from a rigid, perfectly plastic material.

The yield condition proposed by Hodge [22] and illustrated in Fig. 3 will be used in this article since it simplifies considerably a previous analysis,

the results of which agree reasonably well with experimental values recorded on plates loaded impulsively [12]. This approximate yield surface is an "upper" bound to the Tresca yield condition for a uniform shell [23], while a similar one 0.618 times as large provides a "lower" bound.

5. General Equations

Consider a rigid, perfectly plastic circular plate which is simply supported around its outer edge and subjected to an axisymmetrical dynamic load $k(t)$, where $k(t)$ is a function of time and is transverse to the mid-plane of the plate.

Symmetry demands that at $r = 0$

$$m_r = m_\theta = -1 \text{ , and } n_r = n_\theta = 1 \text{ ,} \tag{11}$$

while for $0 \leqslant r \leqslant R$ it may be shown that equations (6)-(10) and a transverse displacement of the form

$$w = W(t)(1 - \frac{r}{R}) \tag{12}$$

are consistent with the flow rule corresponding to the yield condition illustrated in Fig. 3 when

$$m_\theta = -1 \text{ , } n_r = 1 \text{ , } -1 \leqslant m_r \leqslant 0 \text{ and } 0 \leqslant n_\theta \leqslant 1 \text{ .} \tag{13}$$

Substituting equations (10) and (13) into (4) and (5) yields

$$\frac{M_o}{r^2} \frac{\partial}{\partial r} (r^2 m_r') = k(t) - \mu\ddot{w} + \frac{N_o w'}{r} \tag{14}$$

where $k(t)$ is an external load, $\mu\ddot{w}$ is an inertia term, and $N_o w'/r$ is introduced when finite deflections are allowed. It may be shown that when the

$N_o w'/r$ term is disregarded and either $k(t)$ or $\mu\ddot{w}$ or $k(t) - \mu\ddot{w}$ are retained, then equation (14) yields the same results as quoted in references [1,8,7], respectively. If $k(t)$ and $N_o w'/r$ are retained and $\ddot{w} = 0$, then equation (14) predicts results similar to Onat and Haythornthwaite [4] for deflections at $r = 0$ greater than $H/2$. The impulsive loading case in reference [12] was analyzed using equation (14) with $k(t) = 0$, while this article is concerned with dynamic loading for which all three terms must be included.

Substituting equation (12) into (14) and integrating gives

$$\frac{d^2 W(t)}{dt^2} + \gamma^2 W(t) = \delta + \frac{2k(t)}{\mu} \tag{15}$$

where,

$$\gamma^2 = \frac{4p_o}{\mu H}$$

$$\delta = \frac{-2p_o}{\mu}$$

and the constants of integration have been evaluated using the conditions that $m_r = -1$ at $r = 0$, and $m_r = 0$ at $r = R$.

It may be shown, using equations (12) and (14), that

$$m_r{}'' = \frac{k(t)}{3M_o} - \frac{\mu}{M_o} \frac{d^2 W(t)}{dt^2} \left(\frac{1}{3} - \frac{r}{2R}\right) \tag{16}$$

which, using (15), indicates that $m_r{}'' = 0$ at $r = 0$ if

$$\frac{k(t)}{p_o} = 2 + \frac{4W(t)}{H} \tag{17}$$

Thus, if $\dfrac{k(t)}{p_o} > 2 + \dfrac{4W(t)}{H}$, then the yield condition given by equation (13) will be violated and some alternative yield condition must be sought.

6. Rectangular Pressure Pulse $1 \leqslant \lambda \leqslant 2$

The rectangular pressure pulse illustrated in Fig. 1 may be described viz

$$k(t) = k_o \qquad \text{for} \qquad 0 \leqslant t \leqslant \tau \tag{18}$$

and

$$k(t) = 0 \qquad \text{for} \qquad \tau \leqslant t \leqslant T \tag{19}$$

where τ is the duration of a pressure of magnitude k_o and T is the time at which the plate finally comes to rest.

6.1 First Stage $0 \leqslant t \leqslant \tau$

The general solution of equation (15) for this case is

$$W(t) = A \cos\gamma t + B \sin\gamma t + \delta/\gamma^2 + 2k_o/\mu\gamma^2 \tag{20}$$

where the unknown coefficients A and B may be determined from the initial conditions

$$w = \dot{w} = 0 \qquad \text{at} \qquad t = 0 .$$

At the end of the first stage equation (20) gives

$$w = \frac{H}{2} (\lambda - 1)(1 - \cos\gamma\tau)(1 - x) \tag{21}$$

and

$$\dot{w} = \frac{\gamma H}{2} (\lambda - 1)\sin\gamma\tau (1 - x) \tag{22}$$

where $x = r/R$, and $\lambda = k_o/p_o$.

6.2 Second Stage $\tau \leqslant t \leqslant T$

The general solution of equation (15) for this stage is

$$W(t) = C \cos\gamma t + D \sin\gamma t + \delta/\gamma^2 \tag{23}$$

where the unknown constants C and D may be found from the continuity requirements which demand that the displacement and velocity given by equations (12) and (23) at $t = \tau$ should match equations (21) and (22).

Thus,

$$w = \frac{H}{2} [\{(1 + \lambda(\cos\gamma\tau - 1)\}\cos\gamma t + \lambda\sin\gamma\tau\sin\gamma t - 1](1 - x) \qquad (24)$$

but $\dot{w} = 0$ at $t = T$.

Hence,

$$\tan\gamma T = \frac{\lambda\sin\gamma\tau}{1 + \lambda(\cos\gamma\tau - 1)} \qquad (25)$$

and at $t = T$

$$w = \frac{H}{2} [\sqrt{1 + 2\lambda(1 - \cos\gamma\tau)(\lambda - 1)} - 1](1 - x) \qquad (26)$$

which, according to equations (17) and (18), is valid provided $1 \leqslant \lambda \leqslant 2$.

If the w' term is disregarded in equation (14), then it may be shown that

$$w = \frac{H}{4} \lambda\gamma^2\tau^2(\lambda - 1)(1 - x) \quad , \quad \text{at} \quad t = T \qquad (27)$$

which is the same as the result obtained by Hopkins and Prager [7].

7. Rectangular Pressure Pulse $\lambda \geqslant 2$

It has been shown previously that the yield condition given by equation (13) is not suitable for rectangular pressure pulses with $\lambda > 2$. However, a study of the behavior at $\lambda = 2$ suggests that the yield condition given by equation (11) spreads out to some radius $r = \rho_o$, the position of which is related to λ. The behavior of a thin circular plate loaded dynamically with a rectangular pressure pulse having $\lambda \geqslant 2$ can be considered in three stages, viz

1. $0 \leqslant t \leqslant \tau$. $k(t) = k_o$, and a stationary hinge is formed at $r = \rho_o$.

2. $\tau \leqslant t \leqslant T_1$. $k(t) = 0$, and the hinge formed in part 1 travels inwards from $r = \rho_o$ at $t = \tau$ to $r = 0$ at $t = T_1$.

3. $T_1 \leqslant t \leqslant T_2$. $k(t) = 0$, and the hinge remains stationary at $r = 0$ until the plate reaches a permanent position at $t = T_2$.

7.1 First Stage $0 \leqslant t \leqslant \tau$

If τ is small then one might expect that the w' term in equation (14) would only be important in the second and third stages. Therefore, disregarding the w' term in equation (14) and integrating the result with the conditions that $m_r = 0$ at $r = R$ and $m_r = -1$ at $r = \rho_o$, it can be shown that

$$\frac{2}{\lambda} = 1 - \frac{\rho_o}{R} - \left(\frac{\rho_o}{R}\right)^2 + \left(\frac{\rho_o}{R}\right)^3 \tag{28}$$

if,

$$w = \frac{k_o t^2}{2\mu} \quad , \quad \text{for} \quad 0 \leqslant r \leqslant \rho_o \tag{29}$$

and

$$w = \frac{k_o t^2}{2\mu} \frac{(R - r)}{(R - \rho_o)} \quad , \quad \text{for} \quad \rho_o \leqslant r \leqslant R \tag{30}$$

At the end of the first stage $t = \tau$, equations (29) and (30) give

$$w = \frac{k_o \tau^2}{2\mu} \quad , \quad \dot{w} = \frac{k_o \tau}{\mu} \quad , \quad \text{for} \quad 0 \leqslant r \leqslant \rho_o \tag{31}$$

and

$$w = \frac{k_o \tau^2}{2\mu} \frac{(R - r)}{(R - \rho_o)} \quad , \quad \dot{w} = \frac{k_o \tau}{\mu} \frac{(R - r)}{(R - \rho_o)} \quad , \quad \text{for} \quad \rho_o \leqslant r \leqslant R \tag{32}$$

7.2   Second Stage $\tau \leq t \leq T_1$

It may be shown that

$$\dot{w} = \frac{k_o \tau}{\mu} \quad , \quad \text{for} \quad 0 \leq r \leq \rho(t) \tag{33}$$

and

$$\dot{w} = \frac{k_o \tau}{\mu \cdot} \frac{(R - r)}{(R - \rho(t))} \quad , \quad \text{for} \quad \rho(t) \leq r \leq R \tag{34}$$

are consistent with the flow rule for the yield conditions

$$m_r = m_\theta = -1 \; , \quad n_r = n_\theta = 1 \; , \quad \text{when} \quad 0 \leq r \leq \rho(t) \tag{35}$$

and

$$m_\theta = -1 \; , \quad n_r = 1 \; , \quad -1 \leq m_r \leq 0 \; , \quad 0 \leq n_\theta \leq 1 \; , \quad \text{when} \quad \rho(t) \leq r \leq R \tag{36}$$

Equations (33) and (34) are continuous across $r = \rho(t)$ and at $t = \tau$ match the values given by equations (31) and (32) at the end of the first stage.

Substituting equation (34) into (14) and disregarding the w' term, it may be shown that

$$t = \bar{T}_1 \{ 1 - \frac{\rho}{R} - \left(\frac{\rho}{R}\right)^2 + \left(\frac{\rho}{R}\right)^3 \} \tag{37}$$

which suggests that an appropriate form for the time function retaining w' in equation (14) is

$$t = \tau + T_1' \{ 1 - \frac{\rho}{R} - \left(\frac{\rho}{R}\right)^2 + \left(\frac{\rho}{R}\right)^3 - \frac{2}{\lambda} \} \tag{38}$$

Equation (38) gives $t = \tau$ at $\rho = \rho_o$ and

$$T_1 = \tau + T_1' (1 - \frac{2}{\lambda}) \quad \text{when} \quad \rho = 0 \tag{39}$$

where T_1' is an unknown constant, the value of which will be determined later.

Differentiating equation (38) with respect to time gives

$$\frac{1}{R - \rho} = -\frac{T_1' (R + 3\rho)\dot{\rho}}{R^3} \tag{40}$$

In order to analyze the behavior of the plate in this stage, it is convenient to divide it into three separate regions $0 \leqslant r \leqslant \rho(t)$, $\rho(t) \leqslant r \leqslant \rho_o$, and $\rho_o \leqslant r \leqslant R$.

7.2.1 $0 \leqslant r \leqslant \rho(t)$

The deflection w using equations (31) and (33) is

$$w = \frac{k_o \tau^2}{2\mu} + \int_\tau^t \frac{k_o \tau}{\mu} \, dt \tag{41}$$

from which

$$w' = 0 \tag{42}$$

Thus, utilizing equations (33) and (42) equation (14) reduces to

$$\frac{\partial}{\partial r} (r^2 m_r') = 0$$

or

$$m_r = -1 \tag{43}$$

which is consistent with equation (35).

7.2.2 $\rho(t) \leqslant r \leqslant \rho_o$

The transverse displacement w at radius r is

$$w = \frac{k_o \tau^2}{2\mu} + \int_\tau^{t(r)} \frac{k_o \tau}{\mu} \, dt + \int_{t(r)}^t \frac{k_o \tau}{\mu} \frac{(R - r)}{(R - \rho)} \, dt \tag{44}$$

where from (38),

$$t(r) = \tau + T_1'\{1 - \frac{r}{R} - \left(\frac{r}{R}\right)^2 + \left(\frac{r}{R}\right)^3 - \frac{2}{\lambda}\} \qquad (45)$$

Thus, using (40), equation (44) yields

$$w' = \frac{k_o \tau T_1'}{\mu R^3} (R\rho - Rr + \frac{3\rho^2}{2} - \frac{3r^2}{2}) \qquad (46)$$

which, when substituted with the derivative of (34) into (14), yields

$$m_r = \frac{k_o \tau R^2}{12 M_o T_1'(1+3y)(1-y)^3} (2x^2 + \frac{4y^3}{x} - x^3 - \frac{3y^4}{x} - 6y^2 + 4y^3) +$$

$$\frac{k_o \tau T_1'}{6\mu H} (12xy - 4x^2 + 18y^2 x - 3x^3 + \frac{4y^3}{x} + \frac{9y^4}{x} - 12y^2 - 24y^3) - 1 \qquad (47)$$

where, $x = r/R$, $y = \rho/R$, and the constants of integration have been evaluated from the requirement that m_r and m_r' are continuous across $r = \rho$.

7.2.3 $\rho_o \leqslant r \leqslant R$

Now,

$$w = \frac{k_o \tau^2 (R - r)}{2\mu(R - \rho_o)} + \int_\tau^t \frac{k_o \tau (R - r) dt}{\mu(R - \rho)} \qquad (48)$$

and

$$w' = \frac{- k_o \tau^2}{2\mu(R - \rho_o)} + \frac{k_o \tau T_1'}{2\mu R^3} (2R\rho + 3\rho^2 - 2R\rho_o - 3\rho_o^2) \qquad (49)$$

It may be shown, using (34) and (49) that equation (14) gives

$$m_r = \frac{k_o \tau R^2}{12 M_o T_1'(1-y)^3(1+3y)} \left(2x^2 - x^3 + \frac{4y^3}{x} - \frac{3y^4}{x} - 6y^2 + 4y^3\right) -$$

$$\frac{k_o \tau^2 (x-y_o)^2}{\mu H x(1-y_o)} + \frac{k_o \tau T_1'}{6\mu H} \left(12xy + 18xy^2 - 12xy_o - 18xy_o^2 - \frac{4y_o^3}{x} -\right.$$

$$\left. \frac{9y_o^4}{x} + 12y_o^2 + 24y_o^3 + \frac{4y^3}{x} + \frac{9y^4}{x} - 12y^2 - 24y^3\right) - 1 \tag{50}$$

where the constants of integration have been evaluated from the requirement

that m_r and m_r' given by equations (47) and (50) are continuous at $r = \rho_o$.

However, $m_r = 0$ at $x = 1$. Thus,

$$\frac{k_o \tau R^2 (1 - 6y^2 + 8y^3 - 3y^4)}{12 M_o (1-y)^3(1+3y) T_1'} - \frac{k_o \tau^2 (1-y_o)}{\mu H} + \frac{k_o \tau T_1'}{6\mu H} \left(12y + 6y^2 - 20y^3 +\right.$$

$$\left. 9y^4 - 12y_o - 6y_o^2 + 20y_o^3 - 9y_o^4\right) - 1 = 0 \tag{51}$$

which putting $y = 0$ gives

$$C_1 T_1'^2 + C_2 T_1' + C_3 = 0 \tag{52}$$

where

$$C_1 = \frac{k_o \tau}{6\mu H} (-12y_o - 6y_o^2 + 20y_o^3 - 9y_o^4) \tag{53}$$

$$C_2 = \frac{-k_o \tau^2}{\mu H} (1 - y_o) - 1 \tag{54}$$

$$C_3 = \frac{\lambda \tau}{2} \tag{55}$$

Thus,

$$T_1' = \frac{-C_2 \pm \sqrt{C_2^2 - 4C_1 C_3}}{2C_1} \tag{56}$$

and

$$T_1 = \tau + T_1'(1 - \frac{2}{\lambda}) \tag{57}$$

7.3 Third Stage $T_1 \leq t \leq T_2$

The transverse displacement given by equation (12) may be used during this stage because the hinge remains stationary at $r = 0$. However since the relations for w' are given by different expressions across the plate, then it is necessary to divide the plate into two sections $0 \leq r \leq \rho_0$ and $\rho_0 \leq r \leq R$.

7.3.1 $0 \leq r \leq \rho_0$

Using equations (12) and (46) with $\rho = 0$, it may be shown that

$$w' = \frac{-k_0 \tau T_1'}{\mu R^3} (Rr + \frac{3r^2}{2}) - \frac{W(t)}{R} \tag{58}$$

which with equation (12) allows (14) to be rewritten,

$$\frac{\partial}{\partial r} (r^2 m_r') = - \frac{\mu}{M_0} \frac{d^2 W(t)}{dt^2} (r^2 - \frac{r^3}{R}) - \frac{4k_0 \tau T_1'}{\mu R^3 H} (Rr^2 + \frac{3r^3}{2}) - \frac{4W(t)r}{RH} \tag{59}$$

or

$$m_r = - \frac{\mu}{2\rho_0} \frac{d^2 W}{dt^2} (2x^2 - x^3) - \frac{k_0 \tau T_1'}{6\mu H} (4x^2 + 3x^3) - \frac{2Wr}{RH} - 1 \tag{60}$$

where the constants of integration have been evaluated from the condition that $m_r = -1$ at $r = 0$.

7.3.2 $\rho_0 \leq r \leq R$

$$w' = - \frac{k_0 \tau^2}{2\mu(R - \rho_0)} - \frac{k_0 \tau T_1'}{\mu R^3} (R\rho_0 + \frac{3\rho_0^2}{2}) - \frac{W(t)}{R} \tag{61}$$

which, when substituted into equation (14) with (12), yields

$$\frac{\partial}{\partial r} (r^2 m_r') = \frac{-\mu}{M_0} \frac{d^2 W(t)}{dt^2} (r^2 - \frac{r^3}{R}) - \frac{2k_0 \tau^2 r}{\mu(R - \rho_0)H} - \frac{4k_0 \tau T_1'}{\mu R^3 H} (R\rho_0 + \frac{3\rho_0^2}{2})r - \frac{4Wr}{RH} \tag{62}$$

from which it may be shown that

$$m_r = - \frac{\mu}{M_o} \frac{d^2W}{dt^2} \left(\frac{r^2}{6} - \frac{r^3}{12R} + \frac{\rho_o^3}{3r} - \frac{\rho_o^4}{4Rr} - \frac{\rho_o^2}{2} + \frac{\rho_o^3}{3R} \right) - \frac{k_o \tau^2}{\mu H(R - \rho_o)} \left(r + \frac{\rho_o^2}{r} - 2\rho_o \right) -$$

$$- \frac{2k_o \tau T_1'}{\mu R^3 H} \left(R\rho_o + \frac{3\rho_o^2}{2} \right) \left(r + \frac{\rho_o^2}{r} - 2\rho_o \right) - \frac{2W}{RH} \left(r + \frac{\rho_o^2}{r} - 2\rho_o \right) - \left(\frac{1}{r} - \frac{1}{\rho_o} \right) F + G$$

$$(63)$$

where, in order to make m_r and m_r' match equation (60) and its derivative across $r = \rho_o$,

$$F = - \frac{\mu \rho_o^3}{M_o} \frac{d^2W}{dt^2} \left(\frac{1}{3} - \frac{\rho_o}{4R} \right) - \frac{4k_o \tau T_1'}{\mu R^3 H} \rho_o^3 \left(\frac{R}{3} + \frac{3\rho_o}{8} \right) - \frac{2W\rho_o^2}{RH} \qquad (64)$$

and

$$G = - \frac{\mu \rho_o^2}{12M_o} \frac{d^2W}{dt^2} \left(2 - \frac{\rho_o}{R} \right) - \frac{4k_o \tau T_1'}{\mu R^3 H} \rho_o^2 \left(\frac{R}{6} + \frac{\rho_o}{8} \right) - \frac{2W\rho_o}{RH} - 1 \qquad (65)$$

Now if $m_r = 0$ at $r = R$ then it may be shown, using (63)-(65), that

$$\frac{d^2W}{dt^2} + \gamma^2 W = \bar{\delta} \qquad (66)$$

the general solution of which is

$$W = M \cos\gamma t + N \sin\gamma t + \bar{\delta}/\gamma^2 \qquad (67)$$

where

$$\gamma^2 = \frac{4\rho_o}{\mu H} \qquad (68)$$

and

$$\bar{\delta} = - \frac{2\rho_o}{\mu} - \frac{2\rho_o k_o \tau^2}{\mu^2 H} (1 - y_o) - \frac{\rho_o k_o \tau T_1'}{3\mu^2 H} (12y_o + 6y_o^2 - 20y_o^3 + 9y_o^4) \qquad (69)$$

At the beginning of the third stage $t = T_1$, $W = 0$ and the velocity given by equations (12) and (67) must match equation (34) at the end of the second stage.

Hence,

$$W(t) = -\left(\frac{\bar{\delta}\cos\gamma T_1}{\gamma^2} + \frac{k_o\tau\sin\gamma T_1}{\mu\gamma}\right)\cos\gamma t + \left(\frac{k_o\tau\cos\gamma T_1}{\mu\gamma} - \frac{\bar{\delta}\sin\gamma T_1}{\gamma^2}\right)\sin\gamma t + \bar{\delta}/\gamma^2 \tag{70}$$

and

$$\dot{w} = \left(\frac{\bar{\delta}\cos\gamma T_1}{\gamma} + \frac{k_o\tau\sin\gamma T_1}{\mu}\right)\sin\gamma t + \left(\frac{k_o\tau\cos\gamma T_1}{\mu} - \frac{\bar{\delta}\sin\gamma T_1}{\gamma}\right)\cos\gamma t \tag{71}$$

But $\dot{w} = 0$ at $t = T_2$ where,

$$\tan\gamma T_2 = \frac{\dfrac{k_o\tau\cos\gamma T_1}{\mu} - \dfrac{\bar{\delta}\sin\gamma T_1}{\gamma}}{-\dfrac{\bar{\delta}}{\gamma}\cos\gamma T_1 - \dfrac{k_o\tau\sin\gamma T_1}{\mu}} \tag{72}$$

Thus,

$$w = \frac{k_o\tau^2}{2\mu} + \frac{k_o\tau T_1'}{\mu}\left(1 - \frac{2}{\lambda} - \frac{x^2}{2} - \frac{x^3}{2}\right)$$

$$+ \left\{\frac{\bar{\delta}}{\gamma^2} + \left(\frac{\bar{\delta}^2}{\gamma^4} + \frac{k_o^2\tau^2}{\mu^2\gamma^2}\right)^{1/2}\right\}(1 - x), \quad \text{for} \quad 0 \leq x \leq y_o \tag{73}$$

and

$$w = \frac{k_o\tau^2(1 - x)}{2\mu(1 - y_o)} + \frac{k_o\tau(1 - x)T_1'}{\mu}\left(y_o + \frac{3y_o^2}{2}\right)$$

$$+ \left\{\frac{\bar{\delta}}{\gamma^2} + \left(\frac{\bar{\delta}^2}{\gamma^4} + \frac{k_o^2\tau^2}{\mu^2\gamma^2}\right)^{1/2}\right\}(1 - x), \quad \text{for} \quad y_o \leq x \leq 1 \tag{74}$$

At $r = 0$, equation (73) gives

$$w_{max} = -\frac{k_o\tau^2}{2\mu} + \frac{k_o\tau T_1}{\mu} + \frac{\bar{\delta}}{\gamma^2} + \left(\frac{\bar{\delta}^2}{\gamma^4} + \frac{k_o^2\tau^2}{\mu^2\gamma^2}\right)^{1/2} \tag{75}$$

If the w' term is disregarded in (14), then it may be shown that

$$w_{max} = \lambda H\gamma^2\tau^2 (3\lambda - 2)/16, \quad \text{at} \quad t = T_2 \tag{76}$$

which is identical to the result obtained by Hopkins and Prager [7].

8. Discussion

The yield condition [22] indicated in Fig. 3 circumscribes the yield surface of a uniform shell which yields according to the Tresca criterion [23]. A solution which is obtained using this simplified yield condition is termed an "upper" bound while one calculated using a yield surface 0.618 times as large and, therefore, lying everywhere inside the exact yield surface is referred to as a "lower" bound. It is assumed that these "upper" and "lower" bounds would straddle the true solution based on an exact yield surface.

It is clear from the results plotted in Fig. 4 that membrane forces influence considerably the permanent deformation of a simply supported circular rigid-plastic plate loaded dynamically with a rectangular pressure pulse. Hopkins and Prager [7] predict that the final deformation of a plate increases with increase of (k_o/p_o) for a given impulse. However, inclusion of the membrane forces gives rise to a trend in the reverse sense which indicates that membrane forces become increasingly important with increase in λ .

The permanent deformations predicted by the theory presented herein for rectangular pressure pulses of various magnitudes are compared in Fig. 5 with the results obtained from ref. [12] for equivalent impulses. It is evident that a rectangular pressure pulse with $\lambda = 12$ predicts results similar to those presented in [12] for an impulse, while for smaller values of λ , larger deflections are predicted at a given magnitude of I' . It is worth noting in passing that the curves for the impulsive case plotted in Fig. 5 bound closely some experimental results recorded by Florence [14] on Aluminium plates with $R/H = 16$.

9. Conclusions

A theoretical analysis which retains the influence of bending moments and membrane forces has been presented for a simply supported rigid-plastic circular plate loaded with a rectangular pressure pulse. It can be shown that this theoretical analysis predicts final deformations which are considerably smaller than those given by the bending theory of Hopkins and Prager [7] even for maximum deflections only of the order of the plate thickness. It may be shown that a rectangular pressure pulse with $\lambda = 12$ gives a similar maximum permanent deformation to an equivalent impulse, while for smaller values of λ the permanent deflections are larger.

It is thought that the theoretical analysis presented here could be developed further in order to describe the behavior of plates having other support conditions and different characters of loading. However, it is believed that some estimate of the influence of strain-rate effects should be made perhaps in a manner similar to those of Wierzbicki [24] or Perrone [25] who disregarded membrane forces.

References

1. Hopkins, H. G., and Prager, W., "The Load Carrying Capacities of Circular Plates," Journal of Mechs. and Physics of Solids, Vol. 2, No. 1, pp. 1-13, 1953.

2. Drucker, D. C., and Hopkins, H. G., "Combined Concentrated and Distributed Load on Ideally-Plastic Circular Plates," Proc. 2nd U. S. Nat. Cong. App. Mechs., 1954, pp. 517-520.

3. Hu, L. W., "Design of Circular Plates Based on Plastic Limit Load," Journal of Eng. Mechs. Div., Proc. A.S.C.E., Vol. 86, No. EM1, pp. 91-115, 1960.

4. Onat, E. T., and Haythornthwaite, R. M., "The Load Carrying Capacity of Circular Plates at Large Deflection," Jour. App. Mechs., Vol. 23, March 1956, pp. 49-55.

5. Frederick, D., "A Simplified Analysis of Circular Membranes Subjected to an Impulsive Loading Producing Large Plastic Deformations," Proc. 4th Annual Conf. on Solid Mechanics, University of Texas, Austin, Texas, Sept. 1959.

6. Boyd, D. E., "Dynamic Deformations of Circular Membranes," Jnl. Eng. Mech. Div., Proc. A.S.C.E., Vol. 92, No. EM3, June 1966, pp. 1-16.

7. Hopkins, H. G., and Prager, W., "On the Dynamics of Plastic Circular Plates," ZAMP (Jnl. of App. Math. and Physics), Vol. 5, No. 4, 1954, pp. 317-330.

8. Wang, A. J., "The Permanent Deflection of a Plastic Plate Under Blast Loading," Jnl. App. Mech., Vol. 22, 1955, pp. 375-376.

9. Florence, A. L., "Clamped Circular Rigid-Plastic Plates Under Central Blast Loading," Int. J. Solids and Struct., Vol. 2, pp. 319-335, 1966.

10. Witmer, E. A., Balmer, H. A., Leech, J. W., and Pian, T. H. H., "Large Dynamic Deformations of Beams, Circular Rings, Circular Plates, and Shells," AIAA Launch and Space Vehicle Shell Structures Conf., Palm Springs, California, April 1963.

11. Florence, A. L., "Annular Plate Under a Transverse Line Impulse," AIAA Jnl., Vol. 3, No. 9, pp. 1726-1732, Sept. 1965.

12. Jones, N., "Impulsive Loading of a Simply Supported Circular Plate," Brown University Report No. ARPA 37, Feb. 1967.

13. Symonds, P. S., and Mentel, T. J., "Impulsive Loading of Plastic Beams with Axial Constraints," Jnl. Mech. Physics of Solids, Vol. 6, pp. 186-202, 1958.

14. Florence, A. L., "Circular Plate Under a Uniformly Distributed Impulse," Int. J. Solids and Struct., Vol. 2, pp. 37-47, 1966.

15. Symonds, P. S., "Dynamic Load Characteristics in Plastic Bending of Beams," Jour. App. Mech., Vol. 20, No. 4, pp. 475-481, 1953.

16. Perzyna, P., "Dynamic Load Carrying Capacity of a Circular Plate," Arch. Mach. Stos., Vol. 10, No. 5, pp. 635-647, 1958.

17. Hodge, P. G., "The Influence of Blast Characteristics on the Final Deformation of Circular Cylindrical Shells," Jnl. of App. Mech., Vol. 23, pp. 617-624, 1956.

18. Sankaranarayanan, R., "On the Dynamics of Plastic Spherical Shells," Jnl. App. Mech., Vol. 30, March 1963, pp. 87-90.

19. Reissner, E., Proc. Symposia App. Math., Vol. 1, pp. 213-219, 1949.

20. Griffith, J., and Vanzant, H., "Large Deformation of Circular Membranes Under Static and Dynamic Loading," 1st Internat. Cong. on Exptl. Mech., New York, Nov. 1961.

21. Bodner, S. R., and Symonds, P. S., "Experimental and Theoretical Investigation of the Plastic Deformation of Cantilever Beams Subjected to Impulsive Loading," Jnl. App. Mechs., Dec. 1962, pp. 719-728.

22. Hodge, P. G., "Yield Conditions for Rotationally Symmetric Shells Under Axisymmetric Loading," Jnl. of App. Mech., Trans. ASME, June 1960, pp. 323-331.

23. Onat, E. T., and Prager, W., "Limit Analysis of Shells of Revolution," Parts I and II, Proc. Royal Netherlands Acad. of Sci., Vol. B57, pp. 534-541 and 542-548, 1954.

24. Wierzbicki, T., "Dynamic of Rigid Visco-plastic Circular Plates," Arch. Mech. Stos., Vol. 17, No. 6, pp. 851-868, 1965.

25. Perrone, N., "Impulsively Loaded Strain-Rate-Sensitive Plates," J. App. Mech., Paper No. 67-APM-F.

mlw

$$I = k_o \tau$$
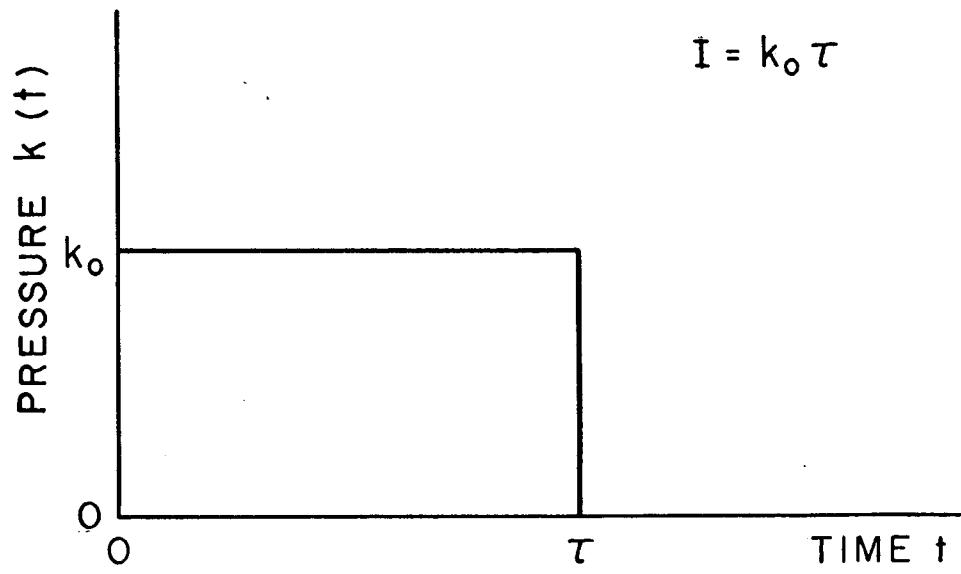
FIG. I RECTANGULAR PRESSURE PULSE
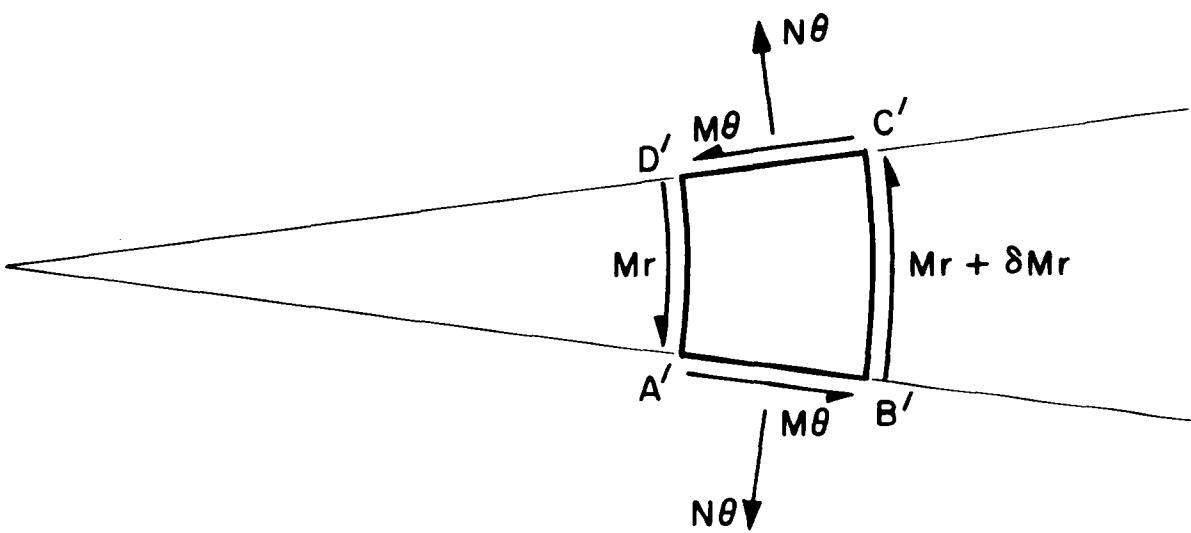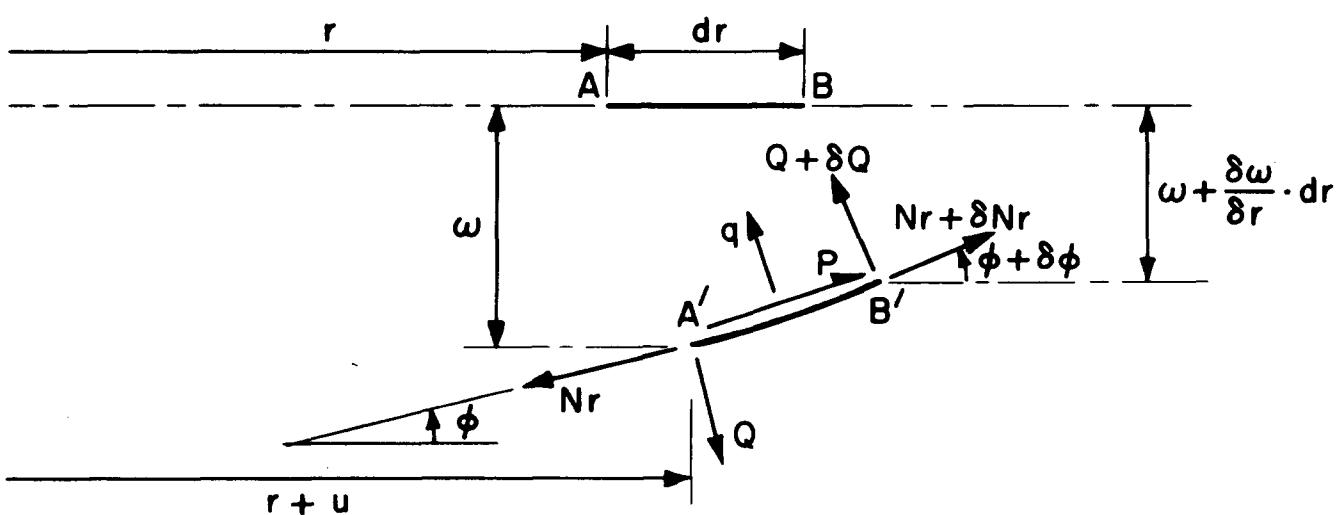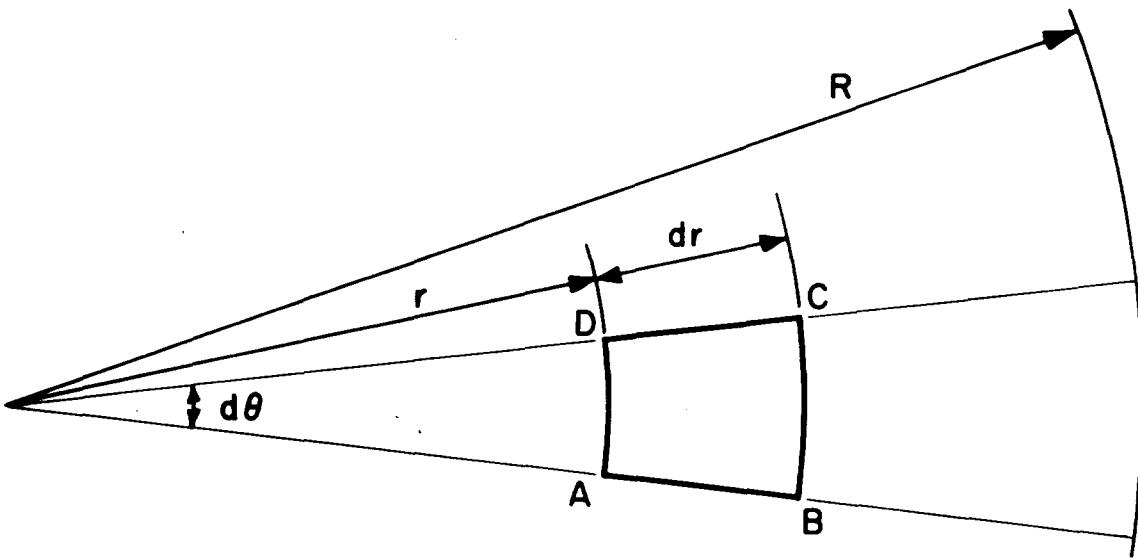
FIG. 2
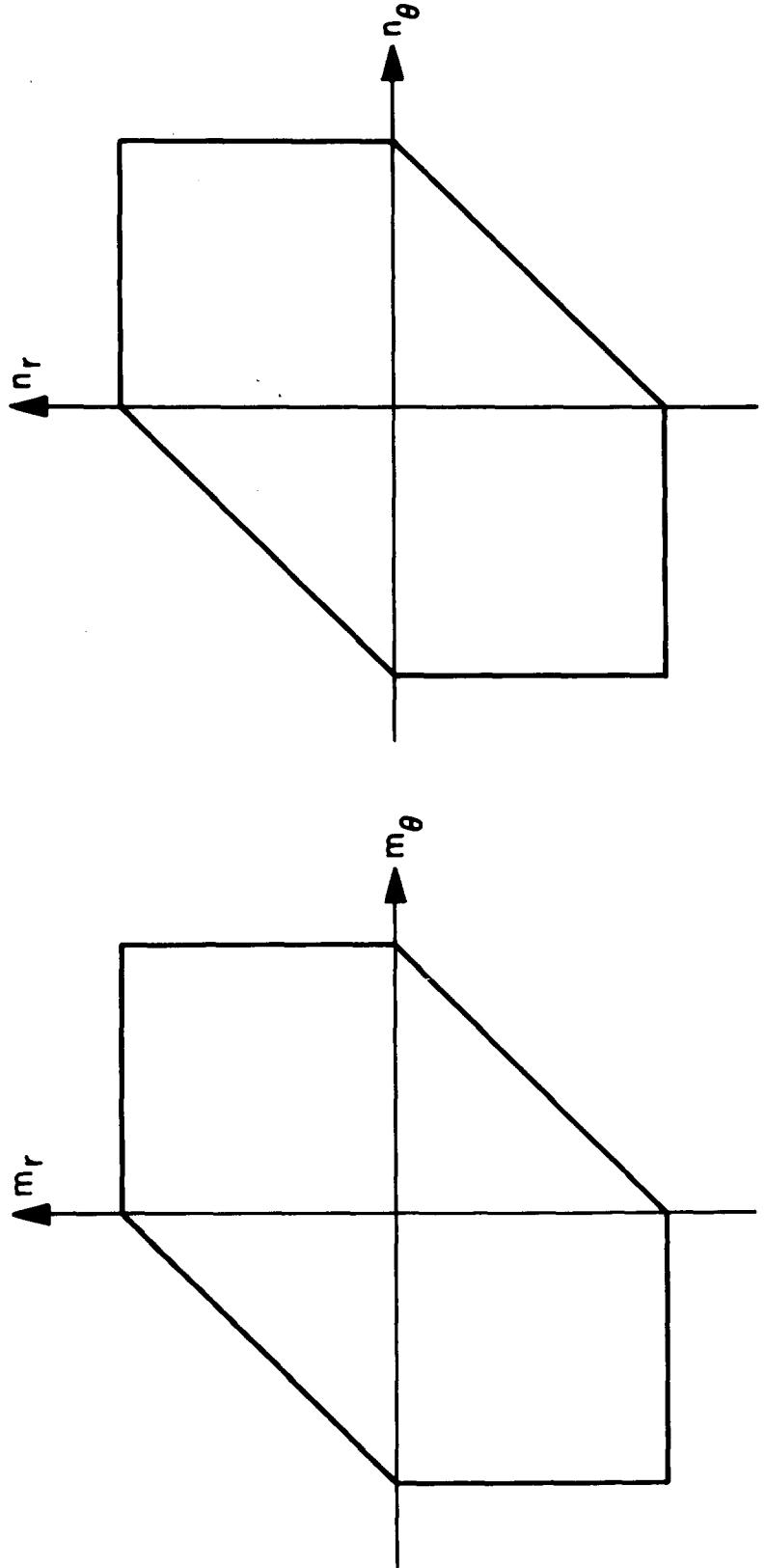
FIG. 3   YIELD CONDITION AFTER HODGE (22)
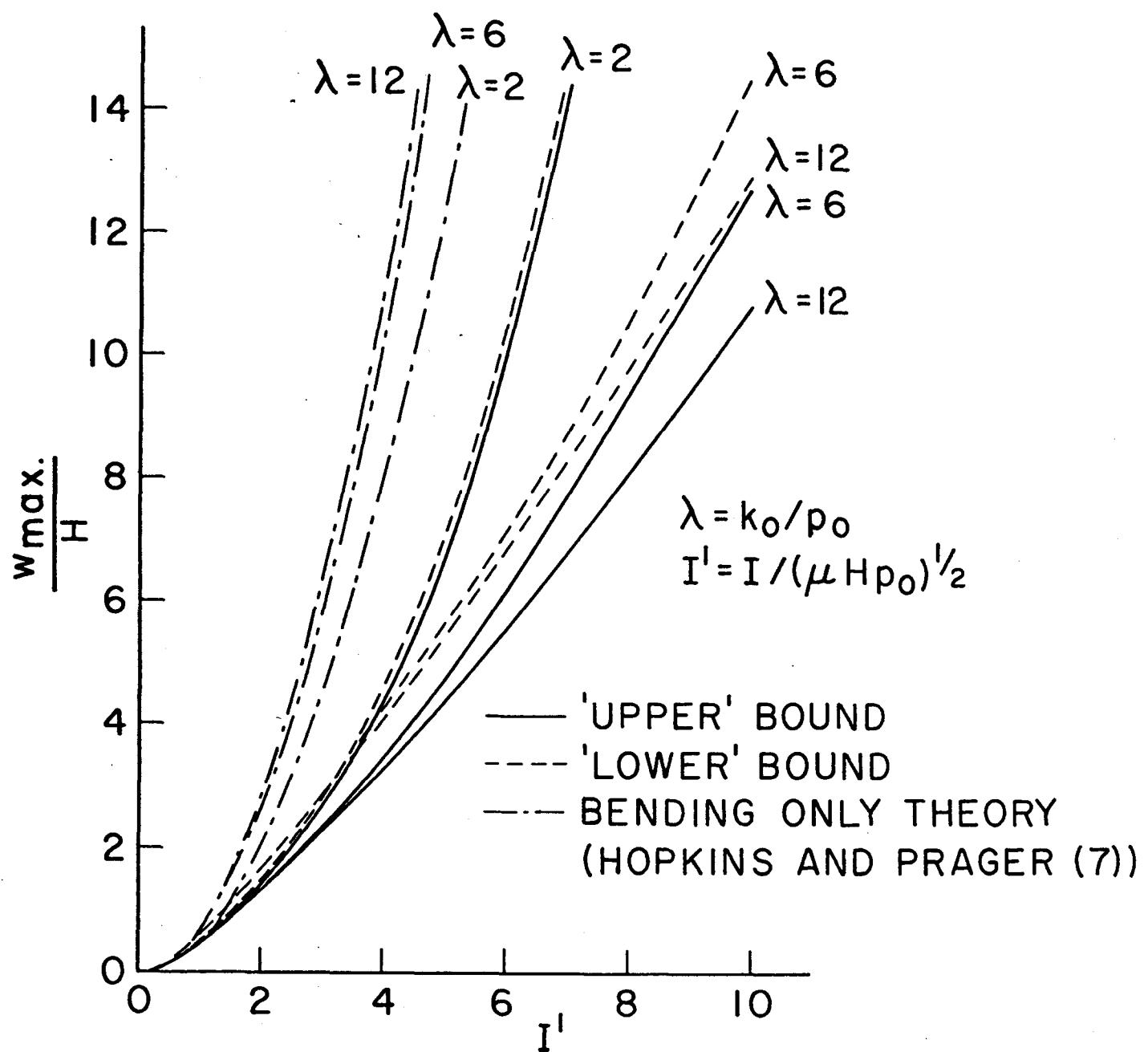
FIG. 4 INFLUENCE OF MEMBRANE FORCES ON THE FINAL DEFORMATION OF A SIMPLY SUPPORTED CIRCULAR RIGID-PLASTIC PLATE SUBJECTED TO A RECTANGULAR PRESSURE PULSE.
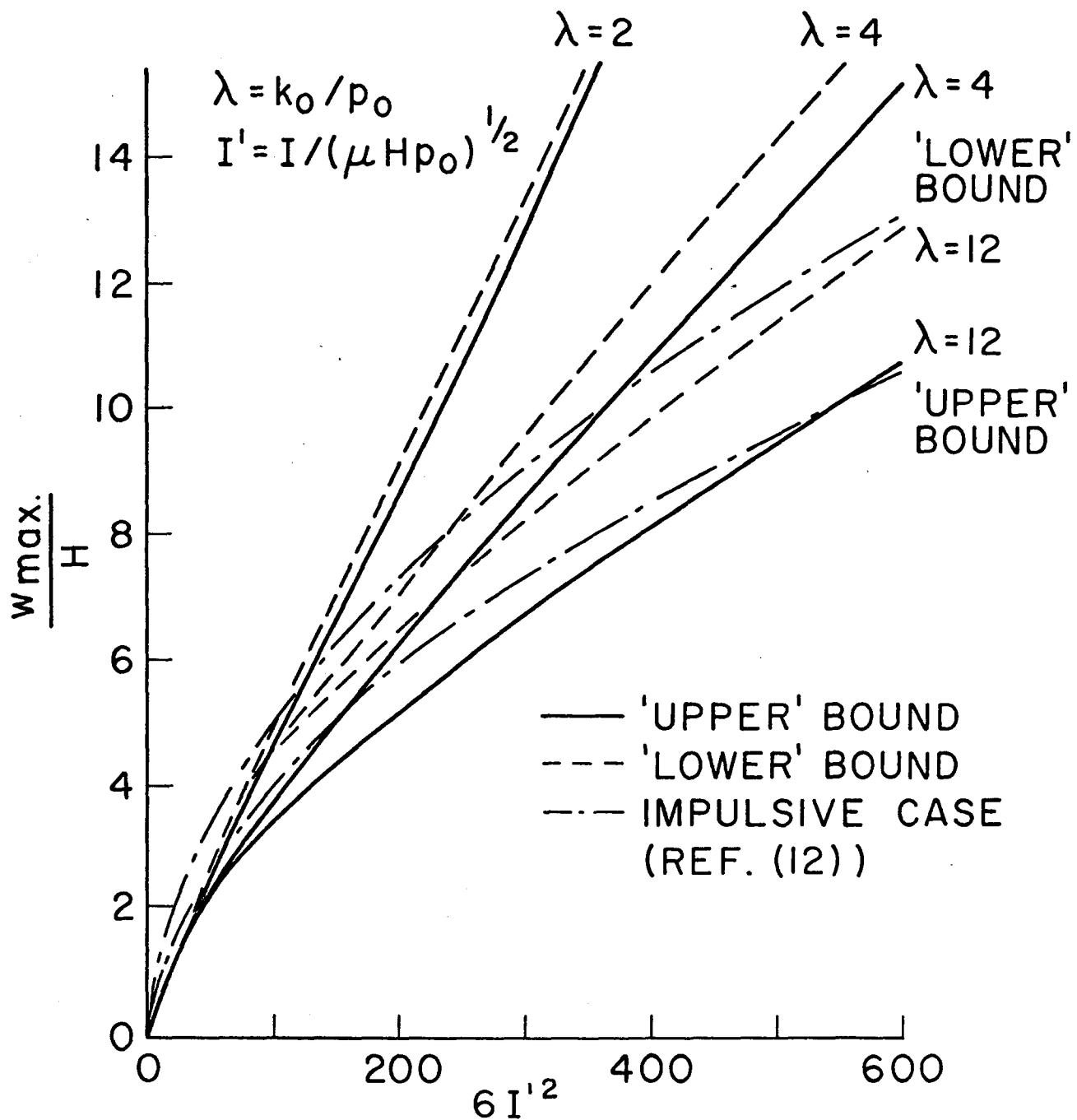
FIG. 5 COMPARISON BETWEEN THE FINAL
DEFORMATIONS OF A RIGID-PLASTIC
CIRCULAR PLATE SUBJECTED TO A
RECTANGULAR PRESSURE PULSE OR AN
IMPULSE.